LETTER

doi:10.1038/nature12329

An Sp1 transcription factor coordinates caspase-dependent and -independent apoptotic pathways

Takashi Hirose[1] & H. Robert Horvitz[1]

During animal development, the proper regulation of apoptosis requires the precise spatial and temporal execution of cell-death programs, which can include both caspase-dependent and caspase-independent pathways[1,2]. Although the mechanisms of caspase-dependent and -independent cell killing have been examined extensively, how these pathways are coordinated within a single cell that is fated to die is unknown. Here we show that the *Caenorhabditis elegans* Sp1 transcription factor SPTF-3 specifies the programmed cell deaths of at least two cells—the sisters of the pharyngeal M4 motor neuron and the AQR sensory neuron—by transcriptionally activating both caspase-dependent and -independent apoptotic pathways. SPTF-3 directly drives the transcription of the gene *egl-1*, which encodes a BH3-only protein that promotes apoptosis through the activation of the CED-3 caspase[3]. In addition, SPTF-3 directly drives the transcription of the AMP-activated protein kinase-related gene *pig-1*, which encodes a protein kinase and functions in apoptosis of the M4 sister and AQR sister independently of the pathway that activates CED-3 (refs 4, 5). Thus, a single transcription factor controls two distinct cell-killing programs that act in parallel to drive apoptosis. Our findings reveal a bivalent regulatory node for caspase-dependent and -independent pathways in the regulation of cell-type-specific apoptosis. We propose that such nodes might act as features of a general mechanism for regulating cell-type-specific apoptosis and could be therapeutic targets for diseases involving the dysregulation of apoptosis through multiple cell-killing mechanisms.

The *C. elegans* pharyngeal M4 motor neuron is generated during embryonic development, whereas the M4 sister cell dies by apoptosis soon after its generation (Fig. 1a)[6,7]. We constructed a $P_{ceh\text{-}28}$*::gfp* reporter transgene that expresses green fluorescent protein (GFP) specifically in the M4 neuron of wild-type animals and in both the M4 neuron and the surviving M4 sister of *ced-3* caspase mutants defective in apoptosis (Fig. 1b)[8], allowing us to identify efficiently mutants defective in M4 sister cell death from a large-scale genetic screen. Among our isolates were two non-allelic mutations—*n4850* and *n4780*—which, on the basis of mapping and transformation-rescue studies, are alleles of the genes *sptf-3* and *pig-1*, respectively (Fig. 1b).

sptf-3 encodes an Sp1 family transcription factor with a characteristic glutamine-rich domain and three C2H2-type zinc finger domains (Fig. 1c). The *n4850* mutant has a single *sptf-3* mutation, at a splice acceptor site of the last exon (Fig. 1c). In total, 34% of *sptf-3(n4850)* mutants had a surviving M4 sister, and this cell-death defect was rescued by a transgene carrying only the *sptf-3* genomic locus (Fig. 1e). A deletion allele of *sptf-3*, *tm607Δ*, and inactivation of *sptf-3* by RNA interference (RNAi) both phenocopied the *sptf-3(n4850)* mutation, demonstrating that a reduction of *sptf-3* function causes a defect in M4 sister cell death (Fig. 1e).

pig-1 encodes an AMP-activated protein kinase (AMPK)-related protein kinase most similar to mammalian maternal embryonic leucine zipper kinase (MELK); *pig-1* is known to regulate the asymmetric cell divisions of several neuroblasts that divide to produce an apoptotic cell, including the M4 sister[4] (Fig. 1d). The *n4780* mutant has a single *pig-1* mutation in the kinase domain, changing a conserved glycine at amino acid 172 to glutamic acid (Fig. 1d). In total, 20% of *pig-1(n4780)* mutants had a surviving M4 sister, and this cell-death defect was rescued by a transgene carrying only the *pig-1* genomic locus (Fig. 1e). A presumptive null allele of *pig-1*, *gm344Δ*, and inactivation of *pig-1* by RNAi both phenocopied the *pig-1(n4780)* mutation, demonstrating that a reduction of *pig-1* function causes a defect in M4 sister cell death (Fig. 1e).

Both *sptf-3* and *pig-1* are required for the deaths of multiple cells, including the sisters of the AQR neuron, the pharyngeal gland cells 1A (g1A) and the pharyngeal I2 interneurons (Fig. 1f). By contrast, neither *sptf-3(n4850)* nor *pig-1(n4780)* affected the deaths of the sisters of the pharyngeal neurosecretory motor (NSM) neurons, the sisters of the pharyngeal I1 interneurons or the ventral C (VC) homologues of the ventral nerve cord (Fig. 1f). Thus, *sptf-3* and *pig-1* seem to promote apoptosis in the same subset of cells fated to die, suggesting that *sptf-3* and *pig-1* have a functional interaction in the regulation of cell death.

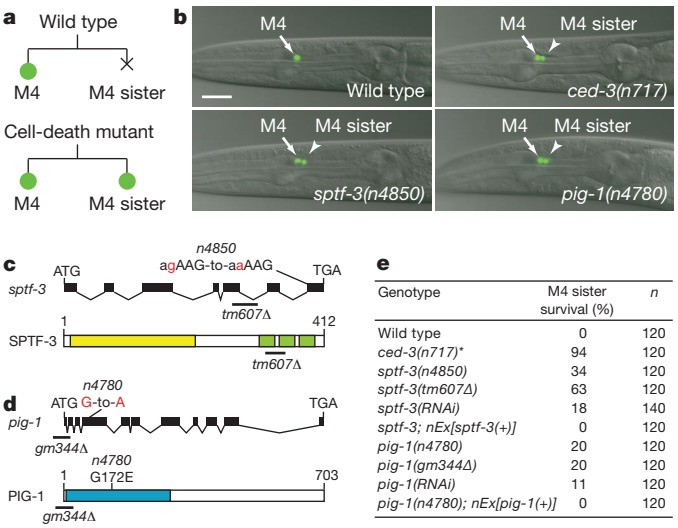

e

Genotype	M4 sister survival (%)	*n*
Wild type	0	120
*ced-3(n717)**	94	120
sptf-3(n4850)	34	120
sptf-3(tm607Δ)	63	120
sptf-3(RNAi)	18	140
sptf-3; nEx[sptf-3(+)]	0	120
pig-1(n4780)	20	120
pig-1(gm344Δ)	20	120
pig-1(RNAi)	11	120
pig-1(n4780); nEx[pig-1(+)]	0	120

f

Genotype	% AQR sister survival (*n*)	% g1A sister survival (*n*)	% I2 sister survival (*n*)	% NSM sister survival (*n*)	% I1 sister survival (*n*)	Extra VC homologues (*n*)
Wild type	0 (50)	0 (240)	0 (120)	0 (240)	0 (240)	0.0±0.0 (120)
ced-3(n717)	54 (50)	99 (240)	100 (40)	*100 (240)	*57 (240)	*4.9±0.3 (120)
sptf-3(n4850)	18 (120)	17 (240)	27 (120)	0 (240)	0 (240)	0.0±0.2 (120)
pig-1(gm344Δ)	16 (120)	16 (240)	49 (120)	0 (240)	0 (240)	0.0±0.0 (120)

Figure 1 | *sptf-3* and *pig-1* promote the death of the M4 sister cell. **a**, Schematic representation of the M4 cell lineage in the wild type and mutants defective in M4 sister cell death. **b**, Merged epifluorescence and Nomarski images of the pharynx in wild-type, *ced-3(n717)*, *sptf-3(n4850)* and *pig-1(n4780)* animals expressing $P_{ceh\text{-}28}$*::gfp*. Scale bar, 20 μm. **c**, **d**, Genomic organizations and protein structures of *sptf-3* (**c**) and *pig-1* (**d**), including the mutations *n4850* and *n4780*. The yellow and green boxes represent the Q-rich and C2H2-type zinc finger domains of SPTF-3, respectively. The blue box indicates the kinase domain of PIG-1. **e**, The percentages of M4 sister survival in animals of the indicated genotypes. **f**, The percentages of survival of the indicated cells and the number of extra VC homologues are shown. Errors are s.d. *Data from ref. 8.

[1]Howard Hughes Medical Institute, Department of Biology, Massachusetts Institute of Technology, 77 Massachusetts Avenue, Cambridge, Massachusetts 02139, USA.

To identify direct transcriptional targets of SPTF-3 involved in the regulation of M4 sister cell death, we performed chromatin immunoprecipitation with massively parallel DNA sequencing (ChIP-seq) analyses using two different SPTF-3 polyclonal antibodies, N81 and M82, both of which specifically recognized the SPTF-3 protein (Supplementary Fig. 1). These experiments identified 2,459 genomic regions that immunoprecipitated with both antibodies (Supplementary Fig. 2a–d and Supplementary Tables 1, 2). Gene ontology analysis indicated that SPTF-3 functions in a variety of biological processes (Supplementary Fig. 2e), consistent with the observation that *sptf-3(n4850)*, the *sptf-3(tm607Δ)* deletion and *sptf-3* RNAi knockdown all cause cell-fate transformations, embryonic and larval lethality and morphological abnormalities (Supplementary Fig. 3 and Supplementary Fig. 4)[9].

We identified an SPTF-3-bound region immediately upstream of the *pig-1* coding region (Fig. 2a). This region contains the consensus SPTF-3 binding motif (CGCCC) identified from our ChIP-seq analyses (Fig. 2b, c). We tested whether the SPTF-3 binding motif of the *pig-1* promoter region is necessary for *pig-1* to promote M4 sister cell death. A wild-type *pig-1* transgene rescued the M4 sister cell-death defect of *pig-1(n4780)* mutants, whereas neither a *pig-1* transgene lacking 71 base pairs of the SPTF-3-bound region of the *pig-1* promoter (Δ71 bp) nor a *pig-1* transgene containing mutations in the consensus SPTF-3 binding motif (mut.1) rescued the M4 sister cell-death defect of *pig-1(n4780)* mutants (Fig. 2d, e). The wild-type *pig-1* promoter expressed GFP in many embryonic cells, whereas mutant *pig-1* promoters lacking the consensus SPTF-3 binding motif (Δ71 bp and mut.1) did not (Supplementary Fig. 5), indicating that the consensus SPTF-3 binding motif of the *pig-1* promoter region is required for *pig-1* expression. Furthermore, *pig-1* transcript levels in *sptf-3(n4850)* mutants were decreased by 43% compared to those of wild-type animals (Fig. 2f), and expression of a $P_{pig\text{-}1}$*::gfp* transgene was frequently absent from the seam cells, P cells, ALM neurons and AVM neuron of *sptf-3(n4850)* mutants (Fig. 2h and Supplementary Fig. 6). Conversely, overexpression of *sptf-3* from a multi-copy transgene under the control of the *sptf-3* promoter induced ectopic expression of *pig-1* in the seam cells and the hyp7 hypodermal cells (Fig. 2g, h). These results indicate that the consensus SPTF-3 binding motif of the *pig-1* promoter region is required for *pig-1* to promote M4 sister cell death and that SPTF-3 is necessary and sufficient for *pig-1* expression, suggesting that SPTF-3 directly drives *pig-1* expression in the regulation of M4 sister cell death.

Although SPTF-3 acts through *pig-1* to promote M4 sister cell death, our genetic observations suggested that *sptf-3* also functions through a pathway distinct from that of *pig-1*. A partial loss-of-function mutation of *sptf-3*, *n4850*, caused a defect in M4 sister cell death more severe than that of the *pig-1* null mutation *gm344Δ* (Fig. 1e). The M4 sister cell-death defect of *sptf-3; pig-1* double mutants is much more severe than that of either single mutant (Supplementary Table 3). Therefore, we tested whether *sptf-3* acts through the pro-apoptotic BH3-only

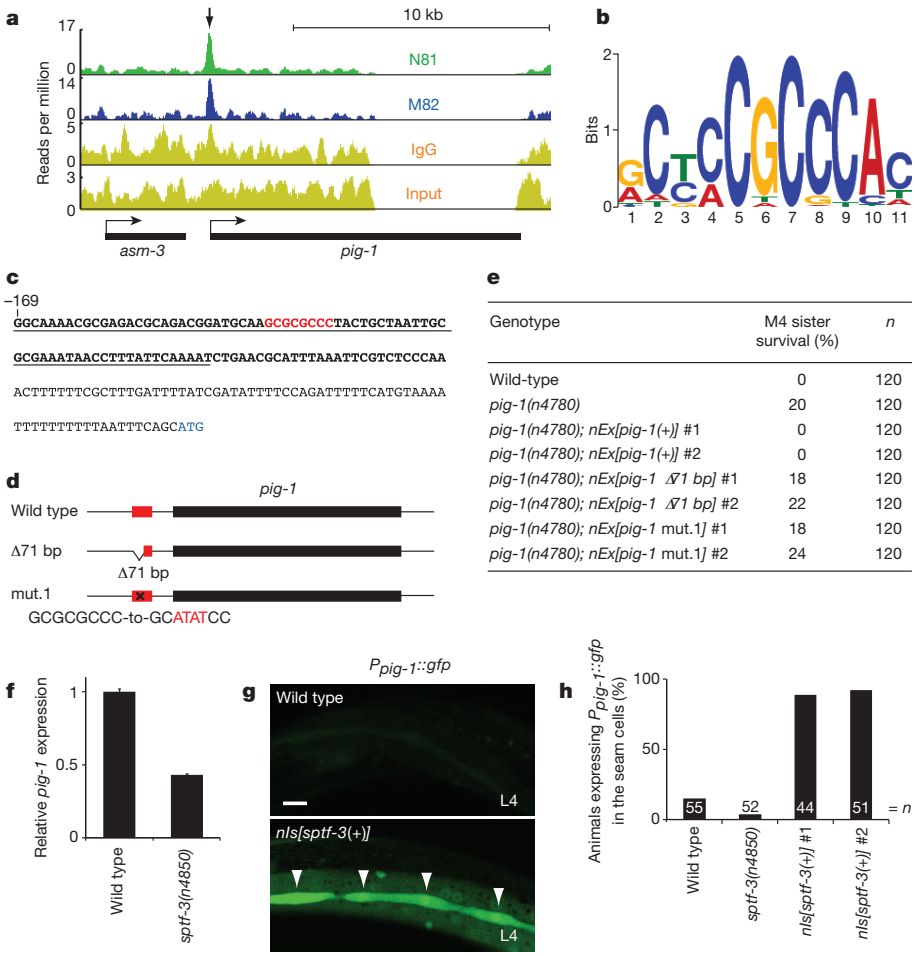

Figure 2 | *pig-1* is a direct transcriptional target of SPTF-3 in the regulation of the death of the M4 sister cell. **a**, ChIP-seq results obtained by immunoprecipitation with the antibodies anti-SPTF-3 N81, anti-SPTF-3 M82 or normal IgG and input chromatin are shown. Arrow, an enriched SPTF-3-bound region. **b**, The consensus SPTF-3 binding motif determined by ChIP-seq is represented. **c**, DNA sequence of the *pig-1* promoter. Bold letters, SPTF-3-bound regions identified by ChIP-seq. Red letters, the GC-rich sequence that contains the consensus SPTF-3 binding motif. Blue letters, the ATG start site of the *pig-1* coding region. Underline, the deleted *pig-1* sequences in the *pig-1*(Δ71 bp) transgene. **d**, Representations of the *pig-1* transgenes used in rescue experiments. Wild-type, a wild-type *pig-1* transgene; Δ71 bp lacks 71 base pairs of the SPTF-3-bound region; mut.1, mutated as shown for the consensus SPTF-3 binding motif. Red box, SPTF-3-bound regions identified by ChIP-seq. **e**, The percentages of M4 sister survival in animals of the indicated genotypes. **f**, *pig-1* messenger RNA levels of wild-type and *sptf-3(n4850)* embryos were measured by quantitative PCR with reverse transcriptase. *pig-1* expression levels of *sptf-3(n4850)* mutants relative to that of the wild type are represented. Error bars, s.d. of three technical replicates. **g**, Expression of $P_{pig\text{-}1}$*::gfp* in animals of the indicated genotypes at the fourth larval stage (L4). Arrowheads, seam cells. Scale bar, 20 μm. **h**, The percentages of L4 larvae expressing $P_{pig\text{-}1}$*::gfp* in the seam cells of animals of the indicated genotypes.

gene *egl-1*, which functions in the caspase-dependent pathway of programmed cell death. *egl-1* acts through the anti-apoptotic *BCL2* homologue *ced-9*, the pro-apoptotic *APAF1* homologue *ced-4*, and the pro-apoptotic caspase gene *ced-3* to drive most cell deaths during the development of *C. elegans*[3]. As *egl-1* is required for M4 sister cell death[8], we scored *egl-1* expression in the surviving M4 sister of *ced-3* mutants defective in apoptosis using a $P_{egl\text{-}1}$*::gfp* reporter transgene that expresses GFP under the control of the *egl-1* promoter[8]. $P_{egl\text{-}1}$*::gfp* was expressed in the M4 sister (100% of animals; $n = 119$) but not in the M4 neuron (0% of animals; $n = 119$) in *ced-3* mutants (Fig. 3a, b), indicating that *egl-1* is not only required for the apoptosis of, but also is expressed in, the M4 sister. We observed that only 33% of *sptf-3(tm607Δ); ced-3* animals expressed $P_{egl\text{-}1}$*::gfp* in the M4 sister, whereas 100% of *pig-1(gm344Δ); ced-3* animals expressed $P_{egl\text{-}1}$*::gfp* in the M4 sister (Fig. 3a, b). Thus, *sptf-3* but not *pig-1* is necessary for normal *egl-1* expression in the M4 sister, suggesting that *sptf-3* acts through both the *egl-1*-mediated apoptotic pathway and the *pig-1*-mediated apoptotic pathway, whereas *pig-1* acts through a pathway distinct from that of *egl-1* to promote M4 sister cell death.

We next asked whether SPTF-3 directly or indirectly drives *egl-1* expression in the M4 sister by examining the *egl-1* promoter region using our ChIP-seq data. We found a small but distinct SPTF-3 binding peak immediately upstream of an *egl-1* coding region (2.77- or 2.96-fold enrichment compared to an input control in the ChIP-seq experiments using SPTF-3 antibody N81 or M82, respectively) (Supplementary Fig. 7a). This SPTF-3-bound region contains two tandem consensus SPTF-3 binding motifs (GGGCGGGGCG) (Supplementary Fig. 7b). These results suggest that SPTF-3 binds to this region. As SPTF-3 regulates *egl-1* expression in a cell-type-specific manner (Fig. 3a and Supplementary Fig. 8) and whole embryos are used for ChIP-seq analyses, it is probable that SPTF-3 binds to the *egl-1* promoter region in only a small number of cells, resulting in a relatively small binding peak.

To test whether the SPTF-3-bound region of the *egl-1* promoter is important for *egl-1* to promote M4 sister cell death, we introduced wild-type and mutant *egl-1* transgenes into *egl-1(n1084 n3082)* mutants defective in M4 sister cell death. A wild-type *egl-1* transgene, pTH01, rescued the M4 sister cell-death defect of *egl-1* mutants, whereas an *egl-1* transgene lacking 30 bp of the SPTF-3-bound region of the *egl-1* promoter did not (Fig. 3c, d). To define further the *egl-1* promoter region important for M4 sister cell death, we introduced a series of mutations into this 30-bp region (Fig. 3c). An *egl-1* transgene containing mutations in the GC-rich sequence (mut.2), in the 9 bp next to the GC-rich sequence at the 5′ side (mut.1), in the 8 bp next to the GC-rich sequence at the 3′ side (mut.3) or in both the GC-rich sequence and the 8 bp next to the GC-rich sequence at the 3′ side (mut.4) all rescued the M4 sister cell-death defect of *egl-1* mutants. By contrast, an *egl-1* transgene containing mutations in both in the GC-rich sequence and 9 bp next to the GC-rich sequence at the 5′ side (mut.5) did not rescue the M4 sister cell-death defect of *egl-1* mutants (Fig. 3d). These results indicate that an *egl-1* promoter sequence containing the consensus SPTF-3 binding motif is required for *egl-1* to promote M4 sister cell death, suggesting that SPTF-3 directly drives *egl-1* expression in the M4 sister.

To further test the hypothesis that SPTF-3 but not PIG-1 functions through *egl-1* in the regulation of M4 sister cell death, we performed epistasis analyses between *sptf-3* or *pig-1* and *ced-9*, which functions downstream of *egl-1*. Because the *ced-9(n2812)* null mutation causes ectopic cell deaths and organismal lethality, we used a weak *ced-3(n2446)* mutation in these experiments to suppress *ced-9(n2812)* lethality (Fig. 3e)[10]. *sptf-3; ced-9* double mutants had nearly the same penetrance of M4 sister survival as that of either single mutant (Fig. 3e). By contrast, *ced-9; pig-1* double mutants were much more highly penetrant for M4 sister survival than either single mutant (Fig. 3e). These results indicate that *sptf-3* and *ced-9* act in a linear pathway and that *pig-1* and *ced-9*, and hence *pig-1* and the caspase gene *ced-3* (considering that *ced-9* acts by regulating *ced-3*) act in parallel in the regulation of the M4 sister cell death, consistent with previous studies that showed that *pig-1* regulates other apoptotic deaths independently of *ced-3* (refs 4, 5). The *C. elegans* genome encodes three additional caspase genes: *csp-1*, *csp-2* and *csp-3*. We observed that *csp-3; csp-1; csp-2* triple mutants were not defective in M4 sister cell death (0% of M4 sister survival; $n = 120$). Because *pig-1* mutants are defective in M4 sister cell death, we conclude that *pig-1* promotes apoptosis of the M4 sister independently of *csp-1*, *csp-2* and *csp-3* and hence through a caspase-independent pathway.

We next tested whether *sptf-3* acts through *pig-1* and *egl-1* to promote apoptosis of other cells, namely the AQR sisters, g1A sisters and I2 sisters, all of which survive in *sptf-3* and *pig-1* mutants (Fig. 1f). The wild-type *pig-1* transgene rescued the defect in apoptosis of the AQR sister, g1A sisters and I2 sisters of *pig-1(n4780)* mutants, whereas the *pig-1* transgene containing mutations in the consensus SPTF-3 binding motif (mut.1) did not (Fig. 4a–c). Thus, the consensus SPTF-3 binding motif of the *pig-1* promoter region is necessary for *pig-1* to promote apoptosis of the AQR sister, g1A sisters and I2 sisters, suggesting that SPTF-3 acts through *pig-1* to promote apoptosis of these cells.

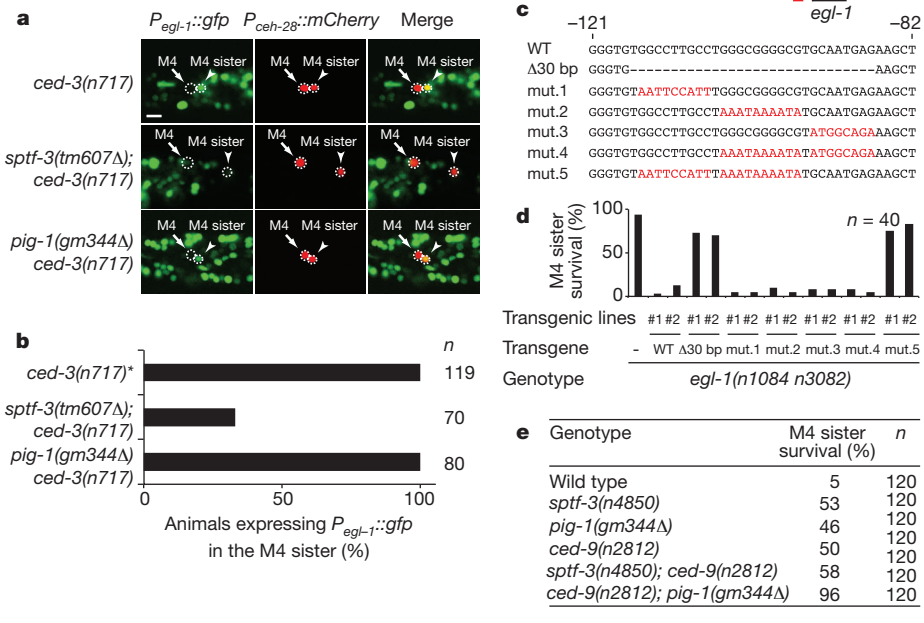

e

Genotype	M4 sister survival (%)	*n*
Wild type	5	120
sptf-3(n4850)	53	120
pig-1(gm344Δ)	46	120
ced-9(n2812)	50	120
sptf-3(n4850); ced-9(n2812)	58	120
ced-9(n2812); pig-1(gm344Δ)	96	120

Figure 3 | *sptf-3* directly drives *egl-1* expression in the M4 sister. **a**, *egl-1* expression in the M4 sister cell of animals of the indicated genotypes. **b**, The percentages of animals expressing $P_{egl\text{-}1}$*::gfp* in the M4 sister of the indicated genotypes. *Data from ref. 8. **c**, Representations of the *egl-1* transgenes used in rescue experiments. WT, a wild-type *egl-1* transgene; Δ30 bp lacks 30 base pairs of the SPTF-3-bound region; mut.1 to mut.5, mutated as shown. Black box, *egl-1*-coding region. Red box, SPTF-3-bound region identified by ChIP-seq. Red letters, mutated bases. **d**, The percentages of M4 sister survival in animals of the indicated genotypes. **e**, The percentages of M4 sister survival in animals of the indicated genotypes. All strains were homozygous for *ced-3(n2446)*.

We also tested whether *sptf-3* acts through *egl-1* to promote apoptosis of these cells. Whereas the *egl-1* transgene pTH01 rescued a defect in apoptosis of the AQR sister but not of the g1A sisters or I2 sisters in *egl-1* mutants, the *egl-1* transgene pBC08 (which overlaps only in part with pTH01) rescued the defect in apoptosis of the g1A sisters and I2 sisters but not of the AQR sister of *egl-1* mutants (Supplementary Fig. 9). Both of these *egl-1* transgenes contain the SPTF-3 binding site required for M4 sister cell death. We therefore tested whether the SPTF-3 binding site is required for *egl-1* to promote apoptosis of the AQR sister using pTH01 and of the g1A sisters and I2 sisters using pBC08. The wild-type pTH01 and pBC08 *egl-1* transgenes rescued a defect in apoptosis of the AQR sister, g1A sisters and I2 sisters of *egl-1* mutants (Fig. 4d–f). The mutant pTH01 *egl-1* transgene (mut.5) containing mutations in the SPTF-3 binding site of the *egl-1* promoter region failed to rescue the defect in apoptosis of the AQR sister of *egl-1* mutants, whereas the mutant pBC08 *egl-1* transgene (mut.5) rescued the defect in apoptosis of the g1A sisters and I2 sisters (Fig. 4d–f). These results indicate that *sptf-3* promotes apoptosis of not only the M4 sister but also of the AQR sister through caspase-dependent and -independent mechanisms through the direct transcriptional activation of *egl-1* and *pig-1*, respectively.

We next determined how *sptf-3* and *pig-1* interact with other genes that specifically regulate M4 sister cell death. We previously reported that the *C. elegans* six family homeodomain protein CEH-34 and the eyes absent protein EYA-1 directly drive the transcription of *egl-1* in the M4 sister to promote M4 sister cell-type-specific apoptosis[8]. *sptf-3(n4850)* synergistically enhanced the M4 sister cell-death defect of *pig-1(gm344Δ)* null mutants, whereas *ceh-34(n4796)* or *eya-1(ok654Δ)* only additively enhanced this defect (Supplementary Table 3). These results indicate that *sptf-3*, *ceh-34* and *eya-1* function in pathways independently of *pig-1*, and that *sptf-3* probably controls *egl-1* at a *cis* regulatory site distinct from that used by the CEH-34–EYA-1 complex in the regulation of M4 sister cell death.

a

Genotype	AQR sister survival (%)	*n*
Wild type	0	120
pig-1(gm344Δ)	16	120
pig-1(gm344Δ); nEx[pig-1(+)] #1	0	120
pig-1(gm344Δ); nEx[pig-1(+)] #2	1	120
pig-1(gm344Δ); nEx[pig-1 mut.1] #1	18	120
pig-1(gm344Δ); nEx[pig-1 mut.1] #2	16	120

b

Genotype	g1A sister survival (%)	*n*
Wild type	0	240
pig-1(gm344Δ)	16	240
pig-1(gm344Δ); nEx[pig-1(+)] #1	0	120
pig-1(gm344Δ); nEx[pig-1(+)] #2	0	120
pig-1(gm344Δ); nEx[pig-1 mut.1] #1	18	120
pig-1(gm344Δ); nEx[pig-1 mut.1] #2	14	120

c

Genotype	I2 sister survival (%)	*n*
Wild type	0	120
pig-1(gm344Δ)	49	120
pig-1(gm344Δ); nEx[pig-1(+)] #1	0	120
pig-1(gm344Δ); nEx[pig-1(+)] #2	1	120
pig-1(gm344Δ); nEx[pig-1 mut.1] #1	42	120
pig-1(gm344Δ); nEx[pig-1 mut.1] #2	40	120

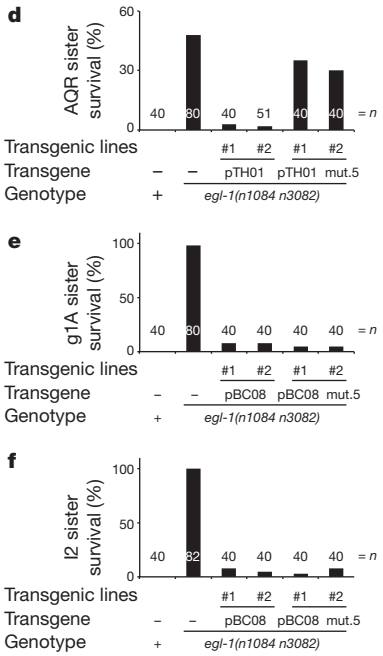

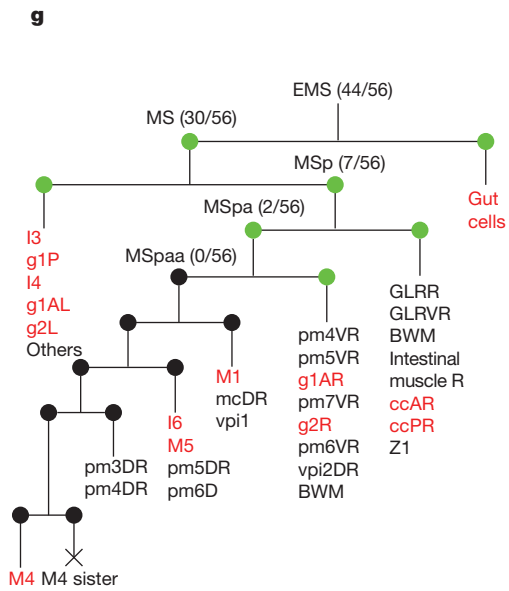

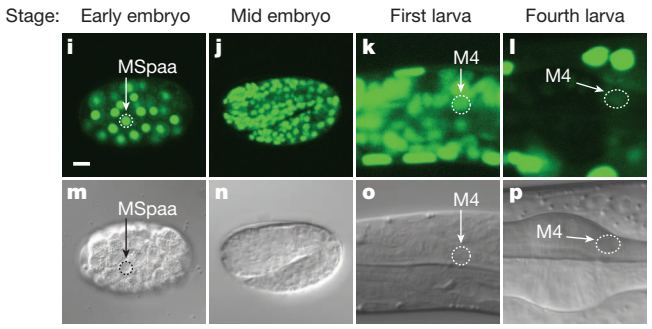

h

Mosaic animal	Cells observed										Cell at which the array lost
	M4	I6	M5	M1	g1AR	g2R	ccAR	ccPR	I3	Gut	
1	–	–	–	–	–	–	–	–	–	–	ND
2	–	–	–	–	–	–	–	–	–	+	MS
3	–	–	–	–	–	–	–	–	+	+	MSp
4	–	–	–	–	–	–	+	+	+	+	MSpa
5	–	–	–	–	+	+	+	+	+	+	MSpaa

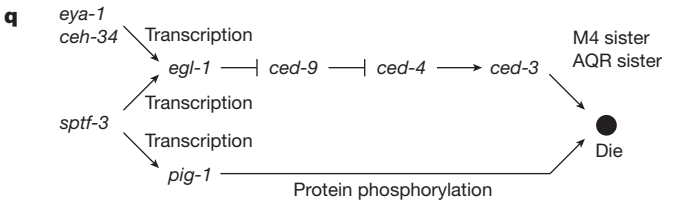

Figure 4 | SPTF-3 functions cell autonomously to promote apoptosis of the M4 sister and the AQR sister. **a**–**f**, The percentages of survival of the AQR sister (**a**, **d**), g1A sister (**b**, **e**) and I2 sister (**c**, **f**) in animals of the indicated genotypes. The *pig-1*(+) transgene carries the wild-type *pig-1* genomic locus, and the *pig-1* mut.1 transgene has mutations in the consensus SPTF-3 binding motif in the *pig-1* promoter region, as described in Fig. 2d. The *egl-1* transgene pTH01 contains 6.5 kilobases (kb) of the 5′ promoter of *egl-1*, the coding region and 2.2 kb of the 3′ of the stop codon of *egl-1*. The *egl-1* transgene pBC08 contains 1.1 kb of the 5′ promoter of *egl-1*, the coding region and 5.7 kb of the 3′ of the stop codon of *egl-1*. pTH01 mut.5 and pBC08 mut.5 have mutations in the consensus SPTF-3 binding motif of the *egl-1* promoter region, as described in Fig. 3c. **g**, Diagram of the M4 cell lineage. The cells in red were scored to determine the cell division at which the *sptf-3*-containing extrachromosomal array was lost in a mosaic animal. Shown are numbers of animals carrying the array in the indicated cell of 56 mosaic animals observed. Green circles, blastomeres in which the array was present. Black circles, blastomeres in which the array was lost. **h**, Examples of mosaic animals carrying an extrachromosomal array in the indicated cells. +, extrachromosomal array present. −, extrachromosomal array absent. **i**–**p**, Nomarski and epifluorescence images of a strain expressing a *gfp::sptf-3* transgene. Scale bar, 10 μm. **q**, A model for the pathways that regulate M4 sister and AQR sister cell-specific programmed cell death.

To identify the cellular site of *sptf-3* action in the regulation of M4 sister cell death, we performed a genetic mosaic analysis (Fig. 4g, h). We generated *sptf-3(n4850)* mutants carrying an extrachromosomal array containing an *sptf-3*-rescuing transgene marked with the cell-autonomous GFP reporters *sur-5::gfp* and *unc-119::gfp* (refs 11 and 12). Extrachromosomal arrays in *C. elegans* are mitotically unstable, resulting in mosaic animals that randomly lose the array in some cell lineages. We observed 56 mosaic animals that were not rescued for the defect in M4 sister cell death but that carried the array with the *sptf-3*-rescuing transgene. Among these 56 animals, we found two animals that retained the array in the blastomere MSpa, the great-great-great-grandmother of the M4 sister (MSpaaaaap), but did not find any animals that retained the array in the blastomere MSpaa, the great-great-grandmother of the M4 sister (Fig. 4g, h), indicating that *sptf-3* is required at or later than the stage of the blastomere MSpaa and seems to function cell autonomously to promote the death of the M4 sister.

To determine the temporal and spatial expression pattern of SPTF-3, we generated a *gfp::sptf-3* transgene that encodes functional SPTF-3, as this transgene rescued the M4 sister cell-death defect of *sptf-3* mutants (data not shown). GFP::SPTF-3 was expressed ubiquitously in embryos and early larval animals (Fig. 4i–k and Supplementary Fig. 10); its expression in the M4 neuron and g1A cells decreased during larval development (Fig. 4k, l and Supplementary Fig. 10a, b). GFP::SPTF-3 was strongly expressed in the seam cells and the hyp7 cells (Supplementary Fig. 10c, d), consistent with the observation that overexpression of *sptf-3* induced ectopic expression of *pig-1* in these cells (Fig. 2g, h). GFP::SPTF-3 localized exclusively to nuclei, consistent with the presumed function of SPTF-3 as a transcription factor. We detected GFP::SPTF-3 expression in MSpaa in embryos (Fig. 4i, m) and in the M4 neuron at the first larval stage (Fig. 4k, o), indicating that the SPTF-3 expression pattern is consistent with our conclusion that *sptf-3* functions cell autonomously to promote the death of the M4 sister.

Given the cell-autonomous function of *sptf-3* and *pig-1* (ref. 4), we tested whether expression of *sptf-3* or *pig-1* could induce apoptosis. Ectopic expression of the caspase CED-3 under the control of the *mec-7* promoter caused the PLM neurons to die, whereas similar expression of either SPTF-3 or PIG-1 failed to do so (Supplementary Fig. 11a). Overexpression of SPTF-3 from a multi-copy array under the control of the *sptf-3* promoter did not result in ectopic apoptosis of the seam cells, M4 neuron, AQR neuron, g1A cells and I2 neurons (Supplementary Fig. 11b, c), all of which normally survive. Consistent with these observations, overexpression of SPTF-3 under the control of the *sptf-3* promoter also did not cause ectopic expression of the pro-apoptotic BH3-only gene *egl-1* (Supplementary Fig. 12), embryonic or larval lethality (Supplementary Table 4). These results indicate that expression of neither *sptf-3* nor *pig-1* is sufficient to promote apoptosis and suggest that other factors are probably required for *sptf-3* or *pig-1* to promote apoptosis.

Our findings demonstrate that the apoptosis of the M4 sister cell is specified by at least two parallel pathways that function non-redundantly: (1) the caspase-dependent apoptotic pathway mediated by *egl-1* and activated through direct transcriptional regulation by two different inputs, by *sptf-3* or by *ceh-34* and *eya-1*; and (2) the caspase-independent apoptotic pathway mediated by *pig-1* and activated through direct transcriptional regulation by *sptf-3* (Fig. 4q). In this apoptotic regulatory network, a single transcription factor, SPTF-3, coordinates caspase-dependent and caspase-independent pathways to promote cell-type-specific apoptosis of the M4 sister and the AQR sister.

Our discovery that there is a common regulatory node for caspase-dependent and caspase-independent apoptosis might identify a general mechanism for the regulation of cell-type-specific apoptosis and, if so, could have an important therapeutic impact, as both caspase-dependent and caspase-independent cell-death processes (such as necroptosis) have been implicated in diseases as diverse as glaucoma, heart attacks and neurodegeneration[13–15]. Our finding that there can be a common regulatory node for the two pathways reveals a new possible approach to therapeutic intervention.

METHODS SUMMARY

C. elegans strains were cultured at 20 °C as described previously[16]. The N2 strain was used as the wild type. The mutations, integrations and extrachromosomal arrays used are described in Methods. *sptf-3(n4850)* and *pig-1(n4780)* were isolated as described[8]. Single nucleotide polymorphisms were used to map *sptf-3(n4850)* and *pig-1(n4780)* to a 136-kb interval (linkage group I: 13,340,839–13,477,415) and a 650-kb interval (linkage group IV: 1–657,968), respectively[17]. For ChIP-seq experiments, ChIP was performed as described[18]. The enriched DNA and input DNA were used to construct libraries for Illumina/Solexa DNA sequencing using HiSeq 2000. The reads were aligned with the *C. elegans* genome using the software Bowtie and analysed as described in Methods. All SPTF-3-bound regions are described in Supplementary Tables 1 and 2.

Full Methods and any associated references are available in the online version of the paper.

Received 18 September 2012; accepted 30 May 2013.
Published online 14 July 2013.

1. Fuchs, Y. & Steller, H. Programmed cell death in animal development and disease. *Cell* **147,** 742–758 (2011).
2. Yuan, J. & Kroemer, G. Alternative cell death mechanisms in development and beyond. *Genes Dev.* **24,** 2592–2602 (2010).
3. Metzstein, M. M., Stanfield, G. M. & Horvitz, H. R. Genetics of programmed cell death in *C. elegans*: past, present and future. *Trends Genet.* **14,** 410–416 (1998).
4. Cordes, S., Frank, C. A. & Garriga, G. The *C. elegans* MELK ortholog PIG-1 regulates cell size asymmetry and daughter cell fate in asymmetric neuroblast divisions. *Development* **133,** 2747–2756 (2006).
5. Denning, D. P., Hatch, V. & Horvitz, H. R. Programmed elimination of cells by caspase-independent cell extrusion in *C. elegans*. *Nature* **488,** 226–230 (2012).
6. Avery, L. & Horvitz, H. R. A cell that dies during wild-type *C. elegans* development can function as a neuron in a *ced-3* mutant. *Cell* **51,** 1071–1078 (1987).
7. Sulston, J. E., Schierenberg, E., White, J. G. & Thomson, J. N. The embryonic cell lineage of the nematode *Caenorhabditis elegans*. *Dev. Biol.* **100,** 64–119 (1983).
8. Hirose, T., Galvin, B. D. & Horvitz, H. R. Six and Eya promote apoptosis through direct transcriptional activation of the proapoptotic BH3-only gene *egl-1* in *Caenorhabditis elegans*. *Proc. Natl Acad. Sci. USA* **107,** 15479–15484 (2010).
9. Ulm, E. A., Sleiman, S. F. & Chamberlin, H. M. Developmental functions for the *Caenorhabditis elegans* Sp protein SPTF-3. *Mech. Dev.* **128,** 428–441 (2011).
10. Hengartner, M. O., Ellis, R. E. & Horvitz, H. R. *Caenorhabditis elegans* gene *ced-9* protects cells from programmed cell death. *Nature* **356,** 494–499 (1992).
11. Yochem, J., Gu, T. & Han, M. A new marker for mosaic analysis in *Caenorhabditis elegans* indicates a fusion between hyp6 and hyp7, two major components of the hypodermis. *Genetics* **149,** 1323–1334 (1998).
12. Maduro, M. & Pilgrim, D. Identification and cloning of *unc-119*, a gene expressed in the *Caenorhabditis elegans* nervous system. *Genetics* **141,** 977–988 (1995).
13. Smith, C. C. T. *et al.* Necrostatin: a potentially novel cardioprotective agent? *Cardiovasc. Drugs Ther.* **21,** 227–233 (2007).
14. Rosenbaum, D. M. *et al.* Necroptosis, a novel form of caspase-independent cell death, contributes to neuronal damage in a retinal ischemia-reperfusion injury model. *J. Neurosci. Res.* **88,** 1569–1576 (2010).
15. Hyman, B. T. & Yuan, J. Apoptotic and non-apoptotic roles of caspases in neuronal physiology and pathophysiology. *Nature Rev. Neurosci.* **13,** 395–406 (2012).
16. Brenner, S. The genetics of *Caenorhabditis elegans*. *Genetics* **77,** 71–94 (1974).
17. Wicks, S. R., Yeh, R. T., Gish, W. R., Waterston, R. H. & Plasterk, R. H. Rapid gene mapping in *Caenorhabditis elegans* using a high density polymorphism map. *Nature Genet.* **28,** 160–164 (2001).
18. Ercan, S. *et al.* X chromosome repression by localization of the *C. elegans* dosage compensation machinery to sites of transcription initiation. *Nature Genet.* **39,** 403–408 (2007).

Supplementary Information is available in the online version of the paper.

Acknowledgements We thank A. Fire, J. Gaudet, C. Barbara and Y. Iino for reporter constructs used to observe cell-type-specific apoptosis; G. Garriga for *pig-1* strains; the *Caenorhabditis* Genetic Center, which is funded by the NIH Office of Research Infrastructure Programs (P40 OD010440) and the National BioResource project for strains; D. Denning, K. Boulias, A. Corrionero and H. Johnsen for comments about the manuscript; and members of the Horvitz laboratory for technical support and discussions. This work was supported by the Howard Hughes Medical Institute. T.H. was supported in part by the Ministry of Education, Science, Technology, Sports and Culture of Japan. H.R.H. is the David H. Koch Professor of Biology at the Massachusetts Institute of Technology and an Investigator of the Howard Hughes Medical Institute.

Author Contributions T.H. and H.R.H. designed the experiments, analysed the data and wrote the manuscript. T.H. performed the experiments.

Author Information Reprints and permissions information is available at www.nature.com/reprints. The authors declare no competing financial interests. Readers are welcome to comment on the online version of the paper. Correspondence and requests for materials should be addressed to H.R.H. (horvitz@mit.edu).

METHODS

***C. elegans* strains and genetics.** *C. elegans* strains were cultured at 20 °C as described previously. The N2 strain was used as the wild type. *sptf-3(n4850)* and *pig-1(n4780)* were isolated as described. Single nucleotide polymorphisms were used to map *sptf-3(n4850)* and *pig-1(n4780)* to a 136-kb interval (linkage group (LG) I: 13,340,839-13,477,415) and a 650-kb interval (LG IV: 1-657,968), respectively. The following mutations, integrations and extrachromosomal arrays were used. LGI: *sptf-3(n4850, tm607Δ), eya-1(ok654Δ), csp-3(n4872Δ), nIs177[P_{ceh-28}::gfp, lin-15AB(+)], zdIs5[P_{mec-4}::gfp, lin-15AB(+)]*. LGII: *csp-1(n4967Δ), nIs343[P_{egl-1}::gfp, lin-15AB(+)]*. LGIII: *ced-9(n2812), nIs176[P_{ceh-28}::gfp, lin-15AB(+)], nIs375[P_{gcy-37}::gfp, lin-15AB(+)], nIs390[P_{flp-15}::gfp, lin-15AB(+)], nIs579[sptf-3(+), P_{myo-3}::mCherry]*. LGIV: *ced-3(n717, n2446), pig-1(n4780, gm344Δ), csp-2(n4871Δ), nIs175[P_{ceh-28}::gfp, lin-15AB(+)], nIs578[sptf-3(+), P_{myo-3}::mCherry], wIs78[ajm-1::gfp, scm::gfp, F58E10, unc-119(+)]*. LGV: *ceh-34(n4796)*. LGX: *lin-15(n765), nIs106[P_{lin-11}::gfp, lin-15AB(+)], nIs283[P_{gcy-10}::gfp, lin-15AB(+)], nIs349[P_{ceh-28}::mCherry, lin-15AB(+)], nIs427[P_{phat-1}::gfp, lin-15AB(+)], nIs429[P_{phat-5}::gfp, lin-15AB(+)], nIs431[gfp::sptf-3], bcIs24[P_{tph-1}::gfp, lin-15AB(+)], nIs540[P_{pig-1}::gfp, rol-6(su1006)]*. Unmapped integrations: *nIs597[P_{pig-1}::gfp, P_{rab-3}::mCherry, sur-5::mCherry, lin-15AB(+)], nIs601 [$P_{pig-1\ \Delta71}$::gfp, P_{rab-3}::mCherry, sur-5::mCherry, lin-15AB(+)], nIs605[$P_{pig-1\ mut.1}$::gfp, P_{rab-3}::mCherry, sur-5::mCherry, lin-15AB(+)]*. Extrachromosomal arrays: *nEx1453* and *nEx1454[sptf-3(+), P_{lin-44}::gfp], nEx1684[sptf-3(+), $P_{unc-119}$::gfp, sur-5::gfp], nEx1971, nEx1972, nEx2105, nEx2106, nEx2109, nEx2110, nEx2113* and *nEx2114 [pig-1(+), P_{lin-44}::gfp], nEx1974* and *nEx1976[pig-1 Δ71 bp, P_{lin-44}::gfp], nEx1978, nEx1979, nEx2107, nEx2108, nEx2111, nEx2112, nEx2115* and *nEx2116[pig-1 mut.1, P_{lin-44}::gfp], nEx1998* and *nEx1999[pTH01 Δ30 bp, P_{lin-44}::gfp], nEx2000, nEx2001, nEx2101* and *nEx2102[pTH01, P_{lin-44}::gfp], nEx2002* and *nEx2003[pTH01 mut.2, P_{lin-44}::gfp], nEx2004* and *nEx2005[pTH01 mut.1, P_{lin-44}::gfp], nEx2006* and *nEx2007 [pTH01 mut.3, P_{lin-44}::gfp], nEx2008, nEx2009, nEx2103* and *nEx2104[pTH01 mut.5, P_{lin-44}::gfp], nEx2010* and *nEx2011[pTH01 mut.4, P_{lin-44}::gfp], nEx2091, nEx2092, nEx2095, nEx2096, nEx2099* and *nEx2100[pBC08, P_{lin-44}::gfp], nEx2093, nEx2094, nEx2098* and *nEx2099[pBC08 mut.5, P_{lin-44}::gfp]*. *nEx2117* and *nEx2118[P_{mec-7}::sptf-3(+), P_{mec-3}::mCherry, rol-6(su1006)], nEx2119* and *nEx2120[P_{mec-7}::pig-1(+), P_{mec-3}::mCherry, rol-6(su1006)], nEx2121* and *nEx2122[P_{mec-7}::ced-3(+), P_{mec-3}::mCherry, rol-6(su1006)]*.

Antibody production. Protein fragments corresponding to amino acids 1–79 and 192–275 of SPTF-3 fused to glutathione *S*-transferase (GST) were expressed, purified using glutathione Sepharose 4B (Amersham Biosciences) and used to raise SPTF-3 N81 and SPTF-3 M82 antibodies, respectively. Antisera were generated by Pocono Rabbit Farm and Laboratory. Polyclonal antibodies were affinity-purified using identical SPTF-3 fragments fused to maltose-binding protein (MBP) and coupled to Affigel 10 (Bio-Rad).

ChIP-seq analysis and bioinformatic analyses. Chromatin immunoprecipitations were performed as described[18]. Wild-type adults were grown on nematode growth medium (NGM) plates, and embryos were obtained by bleaching the gravid adults. Embryos were fixed in 2% formaldehyde for 30 min at room temperature (23 °C), washed once with 100 mM Tris (pH 7.5), twice with M9 buffer and once with FA buffer containing 50 mM HEPES/KOH (pH 7.5), 1 mM EDTA, 1% Triton X-100, 0.1% sodium deoxycholate, 150 mM NaCl with protease inhibitors (Roche), and frozen at −80 °C. In total, 1.7 ml of packed embryos were suspended in 3 ml of FA buffer and homogenized using a dounce homogenizer. The sample was then sonicated using a Branson Sonifier 450 equipped with a microtip in ice water 24 times at the following setting: output control 1.2 and duty cycle constant 30 s ON and 1 min OFF in each cycle. The sample was centrifuged at 13,000*g* for 15 min at 4 °C. The protein concentration of the embryonic extract was determined using a BCA Protein Assay kit (Thermo Scientific). Sarkosyl was added to the embryonic extract at a final concentration of 1%, and the embryonic extract was centrifuged at 13,000*g* for 5 min at 4 °C. Embryonic extract containing 1.54 mg of protein was used as the input control. Embryonic extract containing 15.4 mg of protein and 75 μg of an affinity-purified SPTF-3 N81 antibody, embryonic extract containing 15.4 mg of protein and 54 μg of an affinity-purified SPTF-3 M82 antibody or embryonic extract containing 6.4 mg of protein and 54 μg of normal IgG was incubated at 4 °C overnight for immunoprecipitation in 2 ml of FA buffer containing 1% sarkosyl and protease inhibitors. The precipitated immunocomplexes were collected with Dynabeads protein A (Invitrogen) and washed twice with FA buffer for 5 min, once with FA buffer containing 1 M NaCl for 5 min, once with FA buffer containing 500 mM NaCl for 10 min, once with TEL buffer containing 250 mM LiCl, 1% NP-40, 1% sodium deoxycholate, 1 mM EDTA and 10 mM Tris (pH 8.0) for 10 min and twice with TE buffer (pH 8.0) containing 10 mM Tris (pH 8.0) and 1 mM EDTA for 5 min. The immunocomplexes were eluted twice with 300 μl TE (pH 8.0) containing 1% SDS, 250 mM NaCl and TE at 65 °C for 15 min. The eluted and input samples were incubated at 65 °C overnight to reverse the crosslinking and then treated with 67 μg ml^{-1} of RNase A at room temperature for 1 h followed by 67 μg ml^{-1} of proteinase K at 55 °C for 2 h. DNA was purified by two phenol-chloroform extractions, followed by precipitation with ethanol and re-suspension in 50 μl of H_2O followed by Illumina/Solexa DNA sequencing using HiSeq 2000.

ChIP-seq data analysis. Images acquired from an Illumina/Solexa sequencer were processed through the bundled Solexa image extraction pipeline, which identified polony positions, performed base-calling and generated QC statistics. ChIP-derived reads were aligned with the *C. elegans* genome, Wormbase WS190, using the software Bowtie. Only sequences that mapped uniquely to the genome with zero or one mismatch were used for further analysis. The enriched sites with *P* value $< 10^{-9}$ per antibody defined by ChIP-seq were identified as described[19]. All SPTF-3-bound regions are described in Supplementary Tables 1 and 2.

SPTF-3 binding motif. The sequences for all regions precipitated with an SPTF-3 M82 antibody were analysed using a motif-based sequence analysis tool for large DNA data sets, Multiple Expectation Maximization for Motif Elicitation (MEME)-ChIP[20] (http://meme.sdsc.edu/meme/cgi-bin/meme-chip.cgi) to identify SPTF-3 binding-site motifs. Motifs between six and 30 nucleotides were considered, with a maximum of six motifs for a data set input. The motifs discovered by MEME-ChIP were input to MAST[21] to determine consensus motifs from the MEME-ChIP output and to search a sequence database for sequences that match the motifs.

Gene Ontology analysis. A total of 2,459 SPTF-3-enriched binding regions were identified in ChIP experiments using both the anti-SPTF-3 N81 antibody and anti-SPTF-3 M82 antibodies. Putative target genes with overlapping SPTF-3 binding sites located upstream (≤ 10 kb from the transcription start site) or within the genes were identified, and these genes were subjected to a Gene Ontology enrichment analysis using GOstat[22] (http://gostat.wehi.edu.au/). The complete set of annotated genes was used as the background set of genes.

Plasmid construction. The P_{ceh-28}::*gfp*, P_{ceh-28}::*mCherry*, P_{gcy-10}::*gfp*, P_{egl-1}::*gfp* and wild-type *egl-1* (pTH01 or pBC08) transgenes were described previously[8,23]. The *sptf-3* transgene contained 2.0 kb of 5′ promoter, the coding region and 0.5 kb 3′ of the stop codon in the pGEM-T Easy vector. The *gfp::sptf-3* transgene contained 2.0 kb of the 5′ promoter of *sptf-3*, the *gfp* gene with synthetic introns, the coding region and 0.5 kb 3′ of the stop codon of *sptf-3* in pRS426. The *pig-1* genomic fragment containing 0.8 kb of 5′ promoter, the coding region and 0.6 kb 3′ of the *pig-1* stop codon was cloned into pRS426, and the last intron was removed using two NruI restriction enzyme sites. The QuickChange II XL Site-Directed Mutagenesis Kit (Stratagene) was used to generate the *pig-1*(Δ71 bp) construct lacking the SPTF-3-bound region, the *pig-1* mut.1 construct mutated in the consensus SPTF-3 binding motif, the *egl-1*(Δ30 bp) construct and the *egl-1* mut.1–mut.5 constructs. *sptf-3* complementary DNA was isolated by RT–PCR. The *sptf-3* cDNA fragment corresponding to amino acids 1–79 or 192–275 was cloned in pGEX-4T-3 (GE Healthcare Life Sciences) and pMAL-c2 (New England BioLabs) to express SPTF-3 protein fragments fused with GST or MBP, respectively. The *phat-5* promoter sequence in pGD48, provided from J. Gaudet, was cloned in pPD122.56 to generate the P_{phat-5}::*gfp* transgene. The P_{flp-15}::*gfp* transgene contained 2.4 kb of the 5′ promoter of *flp-15* in pPD122.56. The P_{gcy-37}::*gfp* transgene contained 1.1 kb of the 5′ promoter of *gcy-37* in pPD122.56. For the P_{mec-7}::*sptf-3*, P_{mec-7}::*pig-1* and P_{mec-7}::*ced-3* transgenes, cDNAs containing the entire coding region of each gene were cloned in pPD96.41. The P_{pig-1}::*gfp*, $P_{pig-1(\Delta71\ bp)}$::*gfp* and $P_{pig-1\ mut.1}$::*gfp* transgenes contained 0.9 kb of the 5′ promoter of *pig-1* in pPD122.56. The specific primer sequences are available on request from the authors.

Germline transformation. Germline transformation experiments were performed as described[24]. The *gfp* or *mCherry* transgenes were injected at 50 or 100 μg ml^{-1} into *lin-15(n765*ts*)* or *ced-3(n717) lin-15(n765*ts*)* animals with 50 μg ml^{-1} of pL15EK as a co-injection marker[25]. The *sptf-3* transgene was injected at 10 μg ml^{-1} into *sptf-3(n4850)* animals with 50 μg ml^{-1} of P_{lin-44}::*gfp* as a co-injection marker[26] to rescue the defect in M4 sister cell death. For expression of *sptf-3*, the *sptf-3* transgene was injected at 50 μg ml^{-1} into *nIs540* animals with 5 μg ml^{-1} of P_{myo-3}::*mCherry* as a co-injection marker[27].

Quantitative RT–PCR. Total RNA from wild-type *sptf-3(n4850); nIs349* embryos was prepared using an RNeasy Mini kit (Qiagen). Reverse transcription and quantitative PCR were performed as described[28]. The data presented were generated from three PCR reactions, and *rpl-26* mRNA levels were used for normalization. The specific primer sequences are available on request from the authors.

RNAi analysis. Nucleotides 629–1,238 of the *sptf-3* cDNA and nucleotides 694–2,112 of the *pig-1* cDNA were cloned into the pBluescript II vector, respectively. Sense and antisense RNA molecules were synthesized using T3 and T7 RNA polymerase, respectively, and then annealed to generate double-stranded RNA. The double-stranded RNA was injected into the gonads of *nIs175* adult hermaphrodites, and their progeny were scored at the first larval stage for a defect in M4 sister cell death.

Mosaic analysis. Transgenic animals of genotype *sptf-3(n4850); nIs349; nEx 1684[sptf-3(+), $P_{unc-119}$::gfp, sur-5::gfp]* were generated for the mosaic analysis

experiments. Fifty-six mosaic animals that carried the extrachromosomal array but that were not rescued for the defect in M4 sister cell death were picked and observed using Nomarski optics and epifluorescence to determine the presence or absence of the extrachromosomal array as judged by GFP fluorescence in the following cells: M4, I5, M5, M1, g1AR, g2R, ccAR, ccPR, I3, g1P, I4, g1AL, g2L and intestinal cells. The cell division at which each extrachromosomal array was lost was determined based on the cells that retained the array[7].

Analyses of defects in programmed cell deaths of specific cells. The programmed cell deaths of specific cells were scored at the indicated stages of larval development using the following transgenes, which express GFP in specific cells: M4 sister cell death, *nIs175*, *nIs176* or *nIs177* at the L1 stage; g1A sister cell death, *nIs429* at the L1 stage; I2 sister cell death, *nIs390* at the L4 stage; AQR sister cell death, *nIs375* at the L2 stage; NSM sister cell death, *bcIs24* at the L1 stage; I1 sister cell death, *nIs283* at the L4 stage; VC homologue cell deaths, *nIs106* at the L4 stage. The number of the V-lineage-derived seam cells of young adult animals was scored using *wIs78*, which expresses GFP in the seam cells. A fluorescence-equipped compound microscope was used to score these programmed cell deaths.

Identification of the M4 neuron and the MSpaa cell. The M4 neuron was identified on the basis of its distinctive position in the anterior pharynx. To identify the MSpaa cell, we traced its cell lineage starting from the four-cell-stage embryo, at which point it is possible to easily distinguish the four blastomeres ABa, ABp, P2 and EMS (the progenitor of MSpaa).

19. Marson, A. *et al.* Connecting microRNA genes to the core transcriptional regulatory circuitry of embryonic stem cells. *Cell* **134,** 521–533 (2008).
20. Bailey, T. L. MEME SUITE: tools for motif discovery and searching. *Nucleic Acids Res.* **37,** W202–W208 (2009).
21. Bailey, T. L. & Gribskov, M. Combining evidence using p-values: application to sequence homology searches. *Bioinformatics* **14,** 48–54 (1998).
22. Beissbarth, T. & Speed, T. P. GOstat: find statistically overrepresented Gene Ontologies within a group of genes. *Bioinformatics* **20,** 1464–1465 (2004).
23. Conradt, B. & Horvitz, H. R. The *C. elegans* protein EGL-1 is required for programmed cell death and interacts with the Bcl-2-like protein CED-9. *Cell* **93,** 519–529 (1998).
24. Mello, C. C., Kramer, J. M., Stinchcomb, D. & Ambros, V. Efficient gene transfer in *C. elegans*: extrachromosomal maintenance and integration of transforming sequences. *EMBO J.* **10,** 3959–3970 (1991).
25. Clark, S. G., Lu, X. & Horvitz, H. R. The *Caenorhabditis elegans* locus *lin-15*, a negative regulator of a tyrosine kinase signaling pathway, encodes two different proteins. *Genetics* **137,** 987–997 (1994).
26. Herman, M. A., Vassilieva, L. L., Horvitz, H. R., Shaw, J. E. & Herman, R. K. The *C. elegans* gene *lin-44*, which controls the polarity of certain asymmetric cell divisions, encodes a Wnt protein and acts cell nonautonomously. *Cell* **83,** 101–110 (1995).
27. Frøkjær-Jensen, C. *et al.* Single-copy insertion of transgenes in *Caenorhabditis elegans*. *Nature Genet.* **40,** 1375–1383 (2008).
28. Andersen, E. C., Saffer, A. M. & Horvitz, H. R. Multiple levels of redundant processes inhibit *Caenorhabditis elegans* vulval cell fates. *Genetics* **179,** 2001–2012 (2008).